Active Unit of Solubilized Sarcoplasmic Reticulum Calcium Adenosinetriphosphatase: An Active Enzyme Centrifugation Analysis†

Dwight W. Martin*

ABSTRACT: Sarcoplasmic reticulum calcium adenosinetriphosphatase (Ca^{2+}-ATPase) was solubilized to monomeric form with the nonionic detergent *n*-dodecyl octaethylene glycol monoether ($C_{12}E_8$). Equilibrium ultracentrifugation analysis indicated that this preparation is initially greater than 75% monomer, the remainder being best described as a tetramer. In the presence of substrates, this preparation has ATPase activity comparable to that of leaky sarcoplasmic reticulum vesicles. The possibility of substrate-induced oligomerization of the monomer under ATPase activity assay conditions was tested. Active enzyme centrifugation analysis demonstrated that ATPase activity sedimented with a rate which can only be attributed to a monomeric particle. The sedimentation rate was invariant over a 6-fold concentration range comparable to that used in activity assays. The portion of the protein that sediments as an oligomer when measurements are based on the movement of protein (A_{280}) is not seen when measurements are based on the movement of activity. The data demonstrate that the monomer represents the minimal ATPase active unit of Ca^{2+}-ATPase.

The calcium-dependent ATPase of the sarcoplasmic reticulum (SR)[1] couples ATP hydrolysis to active transport of Ca^{2+} into the SR luminal space (de Meis & Vianna, 1979; Tada et al., 1978). The protein unit of the ATPase has a molecular weight of 119000 ± 6500 (Rizzolo et al., 1976) and comprises up to 90% of the membrane protein of the SR (Meissner, 1975). There is considerable data demonstrating that the ATPase has a tendency to form oligomers within the SR membranes (Vanderkooi et al., 1977; Pick & Racker, 1979; Scales & Inesi, 1976) or in detergent-solubilized systems (le Maire et al., 1976, 1978; Murphy, 1976). However, the functional significance of the oligomeric units remains unknown. It has been suggested that coupling between monomeric units may provide a means of intermolecular regulation and may be obligatory for full activity (Froehlich & Taylor, 1976; Verjovski-Almeida & Inesi, 1979; Ikemoto et al., 1981a,b; Pick & Karlish, 1980; Moller et al., 1980; Watanabe et al., 1981). However, Ca^{2+}-ATPase has also been observed in monomeric form. Hydrolytically active monomeric preparations of the enzyme have been solubilized with detergents (Dean & Tanford, 1978; le Maire et al., 1978; Jorgensen et al., 1978; Murphy et al., 1982; Moller et al., 1980), and a recent liquid X-ray diffraction study indicates that the monomer may be the predominant form in the SR membrane (Brady et al., 1981).

Solubilization of SR Ca^{2+}-ATPase with *n*-dodecyl octaethylene glycol monoether ($C_{12}E_8$) produces a predominantly monomeric preparation which, in the presence of substrates, has ATPase activity comparable to that of leaky SR vesicles (Dean & Tanford, 1978; le Maire et al., 1978). The monomeric character of this preparation has been established by equilibrium ultracentrifugal and hydrodynamic methods (Dean & Tanford, 1978; le Maire et al., 1978). However, these characterizations were conducted in the absence of substrates under conditions in which the enzyme was not hydrolyzing ATP. As such, the species actually responsible for the observed ATPase activity was not *directly* determined. The possibility existed, as recently suggested (Kyte, 1981; Craig, 1982), that under assay conditions, in the presence of a full complement of substrates, the enzyme could oligomerize to form an ATPase active species. Thereby, the solubilized monomer and, by extension, the monomer within the SR membrane would possess only apparent ATPase activity, with the actual active species being a substrate-induced oligomer.

We have tested the hypothesis that monomeric Ca^{2+}-ATPase undergoes substrate-induced oligomerization. On theoretical grounds, using saturating substrate and ATPase monomer concentrations commonly employed under assay conditions, we calculate that dimerization-dependent activity would require bimolecular diffusional rate constants of unprecedented magnitude for protein–protein interactions. Experimentally, we have applied active enzyme centrifugation analysis to Ca^{2+}-ATPase solubilized in $C_{12}E_8$. Our data demonstrate that Ca^{2+}-ATPase solubilized in $C_{12}E_8$ remains monomeric during ATPase enzymatic cycling.

Materials and Methods

Preparation of Solubilized and Delipidated Ca^{2+}-ATPase. Sarcoplasmic reticulum vesicles were prepared from homogenized rabbit skeletal muscle, partially extracted with recrystallized deoxycholate and characterized as previously described (Martin & Tanford, 1981). The leaky vesicles were stored at −20 °C in aliquots containing 2.5 mg of protein (~10 mg/mL).

The leaky vesicles were solubilized and delipidated essentially as described by Dean & Tanford (1978). The $C_{12}E_8$ solubilized preparation, containing 1.37–2.74 M glycerol, was centrifuged in a Beckman airfuge at 30 psig (~178000*g*) for 30 min, 4 °C, and the supernatant containing solubilized protein collected. The delipidated and solubilized Ca^{2+}-ATPase preparation utilized in this study contained ~9 mol of phospholipid per mol of protein based upon organic phosphate content (Bartlett, 1959). Generally, between 33 and 45% of the original leaky vesicle protein was solubilized by the above protocol.

† From the Department of Physiology, Duke University Medical Center, Durham, North Carolina 27710. *Received November 1, 1982.* Supported in part by National Institutes of Health Grant AM04576 (awarded to Dr. Charles Tanford).

* Correspondence should be addressed to this author. He is the recipient of National Research Service Award AM06579.

[1] Abbreviations: AEC, active enzyme centrifugation; ATP, adenosine 5′-triphosphate; $C_{12}E_8$, *n*-dodecyl octaethylene glycol monoether; Ca^{2+}-ATPase, calcium adenosinetriphosphatase; NADH, nicotinamide adenine dinucleotide, reduced; SR, sarcoplasmic reticulum; Tes, *N*-[tris(hydroxymethyl)methyl]-2-aminoethanesulfonic acid; Tris, tris(hydroxymethyl)aminomethane; Mes, 2-(*N*-morpholino)ethanesulfonic acid.

0006-2960/83/0422-2276$01.50/0

ATPase Activity Assays. ATPase activity of the solubilized preparation was assayed by using a modification of the NADH coupled assay of Warren et al. (1974). The assay medium contained 0.01 M Tes, pH 7.5, 0.1 M KCl, 0.1 M $CaCl_2$, 1.5 mM phosphoenolpyruvate, 5 mM Na_2ATP, 5 mM $MgCl_2$, ~0.2 mM NADH, 1.86 mM $C_{12}E_8$, pyruvate kinase (15 IU), and lactate dehydrogenase (36 IU) in a total volume of 1 mL. ATPase activity assays of leaky vesicles used the above medium without $C_{12}E_8$. Activity was assayed by monitoring the loss of OD_{340} of the reaction medium in a thermostatically controlled cell in a Gilford Model 240 spectrophotometer. A Linseis TYP 2041 multichannel recorder equipped with an N42 derivative module was interfaced to the spectrophotometer to allow monitoring of both activity and the rate of loss of activity (slope of the derivatized signal). ATPase activity was also assayed by P_i release according to the protocol of Ottolenghi (1975) and agreed with the value obtained by the coupled assay. ATPase activity of leaky vesicles at 25 °C ranged from 8 to 9.5 μmol min^{-1} mg^{-1} (corresponding to >20 μmol min^{-1} mg^{-1} at 37 °C). Activities of solubilized Ca^{2+}-ATPase at 25 °C ranged from 7 to 9.5 μmol min^{-1} mg^{-1}.

Analytical Ultracentrifugation. Sedimentation equilibrium, sedimentation velocity, and active enzyme centrifugation (AEC) were performed on a Beckman Spinco Model E analytical ultracentrifuge equipped with a photoelectric scanner, an RTIC temperature control unit, and electronic speed control. During equilibrium and velocity sedimentation studies, the absorbance at 280 nm (A_{280}) was used to monitor the protein concentration as a function of the radial distance in the ultracentrifuge cell (r). The density of the solvent was determined on a Mettler/Paar DMA 601M high precision digital density measuring system (Elder, 1979).

For sedimentation equilibrium, glycerol concentration was 1.37–2.74 M and $C_{12}E_8$ concentration was 0.186–1.86 mM, corresponding to $\rho \sim 1.03$–1.06 g/cm^3. A calculated buoyant density factor was used to determine the molecular weight (M_p) of the solubilized protein (Tanford et al., 1974)

$$M_p = \frac{M_p(1 - \phi'\rho)}{(1 - \bar{v}_p\rho) + \delta_d(1 - \bar{v}_d\rho) + \delta_l(1 - \bar{v}_l\rho)} \quad (1)$$

where δ_d and δ_l are the grams of detergent and lipid bound per gram of protein, respectively. For $C_{12}E_8$-solubilized Ca^{2+}-ATPase in low glycerol, $\bar{v}_p = 0.74$ cm^3/g (le Maire et al., 1976), $\bar{v}_d = 0.973$ cm^3/g (Tanford et al., 1977), $\bar{v}_l = 0.975$ cm^3/g (le Maire et al., 1976), $\delta_d = 0.3$ g/g (le Maire et al., 1978), and $\delta_l = 0.06$ g/g. [Preferential hydration of the protein due to the presence of high glycerol (Lee et al., 1979) was ignored since it would change the calculated molecular weight by <±5%.] Sedimentation equilibrium plots (ln A_{280} vs. r^2) showed slight curvature and were analyzed for multicomponent contributions to the total concentration of protein at any position (r) in the cell by standard procedures [e.g., see Schechter et al. (1976)]. In this analysis, $M_p(1 - \phi'\rho)$ for the monomeric unit was determined from the slope of the data near the cell meniscus.

Solvent viscosities were calculated from the glycerol composition. During sedimentation velocity and active enzyme centrifugation studies, glycerol concentration was generally 0.15–0.38 M, and the correction factor for converting the observed s values to $s_{20,w}$ values (Tanford, 1961) was <1.1. In a few sedimentation velocity experiments, glycerol concentration was comparable to that used in sedimentation equilibrium. Under those conditions, the conversion factor to obtain $s_{20,w}$ values was ~1.6–1.8. Comparable $s_{20,w}$ values were obtained at high and low glycerol concentration.

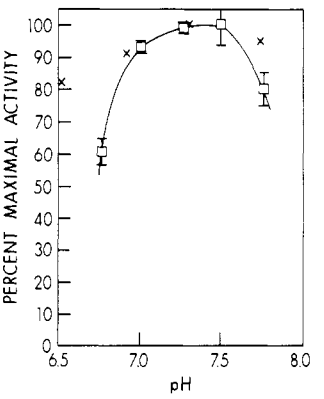

FIGURE 1: pH dependence of ATPase activity of solubilized monomeric Ca^{2+}-ATPase. Activity was determined by assaying P_i release as described under Materials and Methods. The reaction medium was 100 mM KCl, 0.1 mM $CaCl_2$, 5 mM Na_2ATP, 5 mM $MgCl_2$, 1.86 mM $C_{12}E_8$, 50 mM Mes, and 50 mM Tris adjusted to the indicated pH with KOH or HCl. Ca^{2+}-ATPase (final concentration 40 μg/mL) was added to the reaction medium and the mixture incubated for 4 min. Maximal activity at 25 °C was ~6.5 μmol min^{-1} mg^{-1}. (□) Observed activity at the indicated pH; (×) activity at pH 7.5 after a 5-min incubation at the indicated pH. The error bars represent the standard deviation of the mean of triplicate determinations.

Active Enzyme Centrifugation. Active enzyme centrifugation (AEC) was performed according to theories, methods, and precautions generally discussed by Kemper & Everse (1973), Shill et al. (1974), Wei & Deal (1979), Cohen et al. (1967), and Taylor et al. (1972). A band of enzyme is sedimented through a reaction medium such that the generation of product (or loss of substrate) permits the following of band migration with the photoelectric scanner of the ultracentrifuge. The sedimenting band was stabilized (Kemper & Everse, 1973; Taylor et al., 1972) by maintaining the reaction medium at ~2% (v/v) glycerol and the enzyme band initially at ~1% glycerol.

A pH-sensitive dye-linked assay was developed (Shill et al., 1974; Lowry et al., 1954) to follow enzyme activity in the presence of native substrate (MgATP). A major limitation of pH-sensitive assays is that they by definition must be minimally buffered. It is essential to know how the activity of the enzyme will change with pH and whether the change is reversible. Figure 1 shows the ATPase activity of solubilized Ca^{2+}-ATPase as a function of the incubation pH. The activity profile has a limited plateau in the pH range of 7.0–7.6 over which >90% of the maximal activity is observed. On either side of this plateau, there is a precipitous drop in ATPase activity. Activity changes over the indicated pH range were reversible within the error limits of the assay. According to these data, any pH-sensitive assay of activity must be limited to the range of pH 7–7.6.

Total H^+ production during ATP hydrolysis is proportional to P_i production (Nishimura et al., 1962). Measuring H^+ production with a pH indicator dye is best accomplished with systems comprised of a dye and buffer with identical pKs such that changes in absorbance of the dye will be directly proportional to the total H^+ produced during the reaction. This condition was adequately approached by a reaction medium containing 4 mM ATP, 4 mM $MgCl_2$, 0.2 mM Tes, pH 7.6 (pK = 7.5), 0.05 mM bromthymol blue (pK = 7.1; Dean, 1979), 0.186 mM $C_{12}E_8$, 0.274 M glycerol (2% v/v), 0.1 M KCl, and 0.1 mM $CaCl_2$. The absorbance of the above reaction medium at 615 nm changed linearly with total H^+ added (as HCl) over an optical density range of 0.95–0.5, pH ~7.65–7.0 (Figure 2). (A similar linearity was also observed by using a phenol red indicator assay.) The added H^+ needed

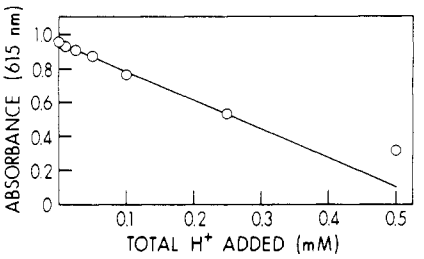

FIGURE 2: A_{615} of the bromthymol blue reaction medium with added H^+. HCl was added to the bromthymol blue linked assay medium (Materials and Methods) to give the indicated H^+ concentration. Absorbance (615 nm) was measured, and the pH of the reaction was subsequently assayed. The reaction medium varied linearly with total H^+ concentration added over an A_{615} range of 0.95–0.5 which corresponds to a pH range of ~7.65–7.0.

to produce this pH change was equivalent to an ~5% hydrolysis of the initial ATP. Therefore, ATP concentration should remain well above saturating levels for Ca^{2+}-ATPase when ATP hydrolysis produces pH changes within this range. The ΔA_{615} of the reaction medium became nonlinear as total H^+ added exceeded 0.25 mM due to the increasing buffering by ATP (MgATP, pK = 5.2; Phillips et al., 1966) at lower pH. Control studies demonstrated that bromthymol blue did not inhibit the ATPase activity of the solubilized enzyme, in agreement with studies of Ca^{2+}-ATPase in SR vesicles (Madeira, 1980). The above pH indicator coupled assay has not proven to be a satisfactory standard assay for ATPase activity as compared to the NADH-coupled or P_i-release assays described earlier. As a standard assay, the pH-sensitive medium requires relatively large amounts of enzyme and has nonlinearity problems associated with the unbuffered nature of the reaction medium. However, initial reaction rates (ΔOD per minute) using the pH indicator assay were approximately proportional to protein concentration, and therefore, the assay meets the minimal requirements for active enzyme centrifugation studies (Cohen et al., 1967; Cohen & Mire, 1971).

The sedimentation of active enzyme was followed by using a double-sector 12-mm Vinograd type I layer forming centerpiece in a cell assembly using sapphire windows. Prior to assembly, 10 μL of enzyme (0.15–0.025 mg/mL) in 1% glycerol, 0.2 mM Tes, pH 7.5, 0.05 mM bromthymol blue, 0.186 mM $C_{12}E_8$, 100 mM KCl, and 0.1 mM $CaCl_2$ was added to the *reference* well of the centerpiece to produce a positive recorder deflection during AEC. (Scans of A_{280} during band centrifugation at higher protein concentration, in reaction medium without ATP, indicated that the initial protein concentration was diluted by a factor of 5–10 soon after being layered onto the reaction medium.) Once assembled, both sectors were filled with 340 μL of reaction medium. The cell was centrifuged at 52000 rpm in an An-D rotor with RTIC set to regulate at 20–21 °C. The cell was scanned at 4-min intervals for the absorbance at 615 nm. Scans (A_{615} vs. centimeters) and derivatized scans (dA_{615}/dt vs. centimeters) were simultaneously recorded with a Linseis multichannel recorder equipped with a derivative module (described above) interfaced to the ultracentrifuge photoelectric scanner. The recorded scans were digitized with a Numonics Corp. Model 1224 electronic digitizer interfaced to a TP-5000 computer system (Tennecomp Systems, Inc.) which uses a PDP 11/05 (Digital Equipment Corp.) as the central processor. Graphics output was provided by a Tektronix 4012 terminal interfaced to a 4610 hard-copy unit (Tektronix, Inc.). Each scan was interpolated into 1024 data points corresponding to 1.61 cm of cell window (i.e., interpolated resolution of ~1.6 μm) and stored in 1023 histographic channels. Scans were smoothed

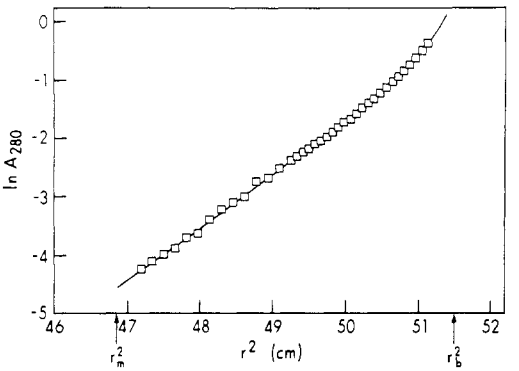

FIGURE 3: Sedimentation equilibrium analysis of $C_{12}E_8$-solubilized Ca^{2+}-ATPase. The initial protein concentration was 0.17 mg/mL in 1.86 mM $C_{12}E_8$ and 1.37 M glycerol. Scans were taken after 36 h at 12000 rpm. r_m and r_b are the distances from the center of rotation of the miniscus and cell bottom, respectively. The line represents a fit to the data by assuming a multicomponent system comprised of ~76% monomer [M_p ~117000, $M_p(1 - \phi'\rho)$ = 27700] and ~24% tetramer. This composition recovered ≥98% of the applied protein. The choice of monomer and tetramer was made after the data were fitted to multicomponent systems of monomer through hexamer.

by using a moving average algorithmn in which each channel is replaced with the average of itself and 24 surrounding channels.

An approximation of the diffusion constant (D) of the active species can be obtained from AEC data by assuming a quasi-Gaussian shape for the difference curves (Claverie, 1980) and equating the variance (σ^2) to the second moment of the activity distribution. The standard deviation (σ) of the distribution was determined from the full width at half-maximum (Γ) according to the relationship $\Gamma = 2.354\sigma$ (Bevington, 1969). This approach avoids contributions from the relatively high noise of the trailing edges of differences curves. The diffusion constant (D) can be related to σ by (Vinograd et al., 1963; Claverie, 1980)

$$\sigma_t^2 = \sigma_0^2 + \left(\frac{s\omega^2\sigma_0^2 + D}{s\omega^2}\right)(e^{2s\omega^2 t} - 1) \qquad (2)$$

where σ_t is the standard deviation of the quasi-Gaussian distribution at time t, σ_0 is the standard deviation at $t = 0$, s is the sedimentation coefficient, and ω is the angular velocity. Accordingly, D is obtained from the slope of a plot of σ_t^2 vs. $e^{2s\omega^2 t} - 1$. The conversion factor to obtain $D_{20,w}$ from D (Tanford, 1961) was ~1.05. The most precise σ_t values were obtained with difference curves which had been smoothed by using a Fourier transform algorithm (FFT),[2] generally utilizing 22 terms in the transform. Fourier transformation improved the precision of σ determination but did not affect the value.

Results

Analytical Ultracentrifugation of Solubilized and Delipidated Ca^{2+}-ATPase. Sedimentation equilibrium of the solubilized protein yielded slightly curved plots of ln A_{280} vs. r^2 as shown in Figure 3 and described previously (Dean & Tanford, 1978; le Maire et al., 1978). Prior studies (Dean & Tanford, 1978) assumed that this curvature was due to a distribution of monomeric and dimeric states. We have applied a more extended multicomponent analysis (see Materials and Methods) to include higher oligomeric states of the protein.

[2] FFT is an adaptation of the routine entitled "FFT 11C—A fast Fourier transform subroutine for complex data" in Decus No. 11-16, the Digital Equipment Computer Users Society, Aug 5, 1971.

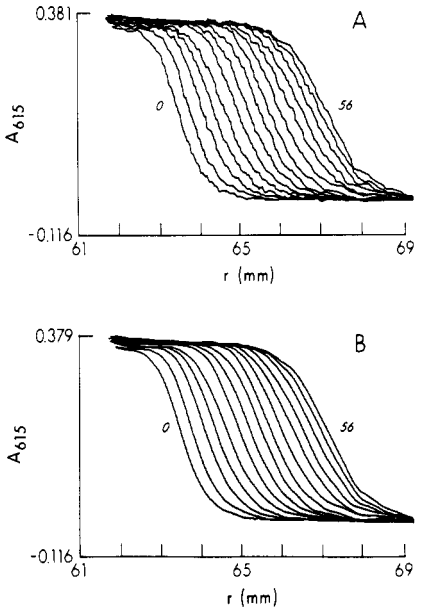

FIGURE 4: Typical scans during active enzyme centrifugation. (A) Successive scans were taken at 4-min intervals. In this data set, the initial protein band concentration was 0.15 mg/mL. r = centrifugal radius. Scans were taken over a 56-min time span, digitized, and stored as described under Materials and Methods. (B) The scans were smoothed by using a moving average as described under Materials and Methods; panels A and B are superimposable.

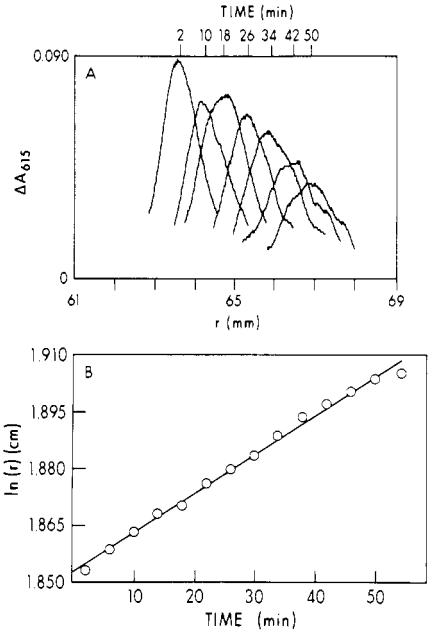

FIGURE 5: (A) Difference curves were derived from successive smoothed scans. For clarity, only the upper 70% of every other difference curve is shown. The upper abscissa gives the activity band center location on the centrifugal radius (r) at the indicated times during centrifugation. The activity band center was determined by the center of area under the upper half of the difference curves. (B) Time-dependent migration of activity band. Data obtained as described in Figure 5A were used to generate the above semilog plot. The slope of the least-squares fit to the data was used to determine the sedimentation rate constant.

This analysis assumes noninteraction between states of the protein. A value of ~27 000 for $M_p(1 - \phi'\rho)$ (corresponding to M_p ~117 000) was obtained from a linear fit to the first several data points near the miniscus. Our analysis indicated a protein composition of >75% monomer. The remaining protein (>20%) is best described as tetrameric with dimeric and trimeric species making insignificant (<5%) contributions to the total protein of the sample. The inclusion of pentamers and hexamers in the model did not improve the fit to the data. The results of several analyses indicate that this preparation is generally comprised of 75–90% monomer.

Sedimentation velocity analysis of delipidated and solubilized Ca^{2+}-ATPase yielded $s_{20,w}$ values of ~5.2 S. This value falls within the range reported by others for monomeric Ca^{2+}-ATPase, 4.8–6.5 S (Jorgensen et al., 1978; le Maire et al., 1976, 1978; Moller et al., 1980). Preparations which had been stored for a few days at 4 °C yielded scans with poorly defined boundaries, indicating formation of higher oligomers.

ATPase Activity of Solubilized and Delipidated Ca^{2+}-ATPase. When the NADH-coupled ATPase assay was used, maximal activity was observed immediately upon recording ΔA_{340} (after a 5–10-s mixing period) and occurred without a time lag. Activity measurements were generally made at enzyme concentrations of 1–5 μg/mL (~10–50 nM). In contrast to the leaky vesicle system, ATPase assays of solubilized and delipidated Ca^{2+}-ATPase did not produce a constant slope of ΔA_{340} per minute during the recording of an assay. The apparent V_{max} decreased from an initial maximum. As a first approximation, the rate of activity loss was fitted to a pseudo-first-order model and found to be 0.01–0.05 min^{-1} at 20 °C (0.07–0.15 min^{-1} at 37 °C). These rates of activity loss agree with the observations of Moller et al. (1980) on a $C_{12}E_8$-solubilized Ca^{2+}-ATPase preparation. The activity loss during assay was mainly related to enzymatic cycling and not protein dilution or surface denaturation in the assay cuvette. The specific activity, based upon the initial velocity, of the solubilized and delipidated protein was approximately the same as that of the leaky vesicles from which it originated and typically ranged between 18 and 23 μmol min^{-1} mg^{-1} at 37 °C.

Active Enzyme Centrifugation. Active enzyme centrifugation was conducted over an initial protein concentration range of 0.025–0.15 mg/mL. Figure 4A shows scans taken durng one experiment. The signal from the photoelectric scanner has a high level of noise at 615 nm. This noise is amplified upon generating difference or derivative curves. Therefore, the scans were smoothed as described under Materials and Methods and shown in Figure 4B. Smoothing did not change the relative positions of the scans, and the scans of panels A and B of Figure 4 are superimposable. Difference curves were derived from successive smoothed scans as shown in Figure 5A. The area under the difference curves was dependent upon the initial protein concentration and the specific activity of the preparation at the time of the analysis. The area decreased during the course of an AEC experiment with a rate of ~0.01 min^{-1} which is consistent with the rate of loss of activity during enzymatic cycling.

The decreasing activity of the preparation during AEC precluded the use of half-boundary height analysis for determination of the sedimentation constant (Llewellyn & Smith, 1978). However, the radial locations (r) of the center of mass of product distributions obtained from derivative or difference curves are relatively insensitive to small activity losses and may be used to obtain linear semilog plots for sedimentation rate determination. The activity band radii (r) were determined from the center of area under the upper half of the difference curves. This method gave the best precision in the determination of s, but the same sedimentation rate was obtained when the activity band radii (r) were defined by either the half-width at half-height or the maxima of the difference curves. The activity band radii (r) were obtained from derivative curves by the center at half-height (data not shown). Figure 5B shows a semilog plot of activity sedimentation. The slope of the plot

Table I: Effect of Protein Concentration on Active Enzyme Sedimentation

initial protein concn (mg/mL)	sedimentation rate (10^{-13} s^{-1}) BB[a]	PR[b]
0.025	5.6	
0.05	5.5	5.3
0.10	5.5	5.0
0.15	5.7	

[a] Data obtained by using bromthymol blue indicator assay as described under Materials and Methods. [b] Data obtained by using a phenol red indicator assay system of the same substrate composition as the bromthymol blue system described under Materials and Methods.

was used to determine the sedimentation rate (Tanford, 1961).

Sedimentation coefficients determined by active enzyme centrifugation as a function of protein concentration are given in Table I. Results obtained by using a phenol red pH indicator linked assay are also included (data not shown). Correction for viscosity, density, and temperature yielded $s_{20,w}$ values of 6.1 ± 0.3 S and 5.4 ± 0.2 S from AEC data obtained with bromthymol blue and phenol red assays, respectively. Within the 5–15% error reported for this method (Cohen et al., 1967; Kemper & Everse, 1973), the $s_{20,w}$ obtained by AEC agrees with that obtained in sedimentation velocity studies of noncycling monomer. The sedimentation coefficient obtained by AEC was constant over a 6-fold concentration range (higher concentrations were not studied). Taken together, the only consistent interpretation is that activity sediments as a monomer.

Sedimentation velocity of total protein (A_{280}) performed 3 days after solubilization yielded poorly defined boundaries. Five days after solubilization, sedimentation velocity analysis of total protein was not possible due to the highly heterogeneous and aggregated nature of the sample. However, the sedimentation rate of enzymic activity was unchanged 7 days after solubilization. The activity boundary remained well-defined regardless of the storage time. The stability and tendency to aggregate have been variable between solubilized preparations, with some preparations producing $s_{20,w}$ values of the total protein (A_{280}) of 5–6 S after 7 days of storage. However, the $s_{20,w}$ value obtained by AEC was independent of the degree of total protein aggregation. These data demonstrate that the aggregates do not sediment as active species in the presence of substrates.

The assumption of a Gaussian shape for the difference curves was tested by calculating the skewness coefficient (α):

$$\alpha = \frac{m_3}{m_2^{3/2}} \tag{3}$$

where m_2 and m_3 are the second and third moments about the mean of the distribution (Remington & Schork, 1970). Analysis of 92 difference curves yielded a mean skewness of $\alpha = 0.36 \pm 0.24$, which falls within the 95th percentile confidence levels for a normal distribution. Skewness did not follow any reproducible trend over the entire time course of centrifugation. In some experiments, skewness decreased somewhat during the first few difference curves (e.g., Figure 5A); however, a trend toward increasing skewness was never observed. A slightly larger α in the early time distributions may be related to a loading anomaly produced by layering the sample buffer (without ATP) onto the reaction medium. This causes a small ΔA_{615} near the miniscus which is independent of the enzyme. Skewness decreases as the band migrates out of this zone. However, even within this zone, skewness was

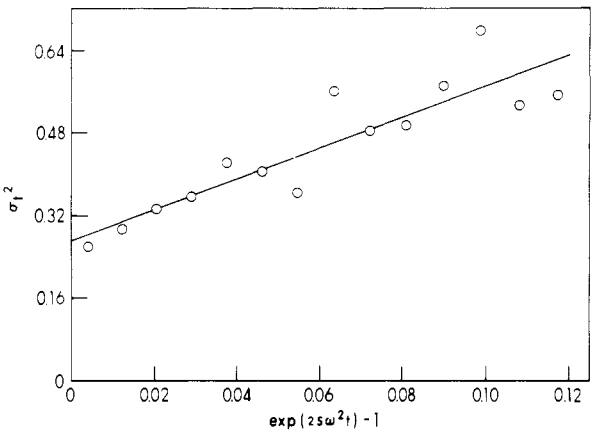

FIGURE 6: Determination of the diffusion constant from AEC data of enzymatically cycling solubilized Ca^{2+}-ATPase. The σ_t for each difference curve was determined from the width at half-height as described in the text. Successive σ values were obtained from the same AEC experiment and plotted as shown according to eq 2. A linear least-squares fit to the data yielded slope = (2.98 ± 0.44) × 10^{-2} cm^2, σ_0^2 = (0.27 ± 0.03) × 10^{-2} cm^2, and linear correlation coefficient = 0.8910. The diffusion coefficient, calculated as described under Materials and Methods, is $D = (4.6 \pm 0.9) \times 10^{-7}$ cm^2 s^{-1}.

Table II: Summary of Analysis

method	$s_{20,w}$ (10^{-13} s^{-1})	$D_{20,w}$ (10^{-7} cm^2 s^{-1})	M_p
sedimentation velocity	5.2 ± 0.3	4[a]	117 000 ± 6 700
AEC[b]	5.8 ± 0.5	5 ± 1	104 000 ± 23 000

[a] From le Maire et al. (1978); no error given. [b] Mean and standard deviations of values obtained by bromthymol blue and phenol red assay systems.

generally within the limits of a Gaussian distribution. Slight skewing may be expected in band centrifugation since the leading edge experiences a greater centrifugal force due to its greater radial distance from the axis of rotation (Vinograd & Bruner, 1966). Although skewness was generally small and positive, occasional negative skewness was observed. The sedimentation rate of the center of mass of the entire distribution agreed within 2% with the rate obtained from the center of mass of the upper half-height. Taken together, these data demonstrate that the Gaussian assumption is a good approximation to the shape of the difference curves and that the active enzyme band is essentially monodisperse.

The diffusion constant (D) of the active species was determined from AEC data as described under Materials and Methods (Figure 6). The results of seven analyses yielded $D_{20,w} = (5 \pm 1) \times 10^{-7}$ cm^2 s^{-1}. This compares to $D_{20,w} = 4 \times 10^{-7}$ cm^2 s^{-1} for $C_{12}E_8$-solubilized monomeric Ca^{2+}-ATPase not undergoing enzymatic cycling (le Maire et al., 1978). The particle molecular weight is related to the diffusion constant and the sedimentation rate constant by the Svedberg relation (Tanford, 1961).

$$M_p(1 - \phi'\rho) = \frac{skTN}{D} \tag{4}$$

The results of sedimentation velocity analysis of noncycling monomeric enzyme and AEC analysis are summarized in Table II. The M_p calculated in Table II is relatively insensitive to δ_d (a value of 0.3 g/g was used in the table); e.g., at δ_d = 1, M_p is reduced by <7%. Additionally, the discrepancy between $D_{20,w}$ for cycling and noncycling enzyme is not enough to change the interpretation (i.e., with $D_{20,w} = 4 \times 10^{-7}$ cm^2/s, AEC data yield M_p = 130 000). The only consistent inter-

pretation is that activity sediments as a monomer.

Discussion

The central aim of this study was to unequivocally determine if the solubilized monomer possesses ATPase activity. Equilibrium and hydrodynamic analyses of $C_{12}E_8$-solubilized Ca^{2+}-ATPase demonstrate that this preparation is largely monomeric although upon solubilization there is initially a small (<30%) and variable amount of oligomeric species. Given the high specific activity of the solubilized and delipidated preparation, it is difficult to attribute the ATPase activity solely to the oligomer initially present after solubilization. For this to be true, the V_{max} of the solubilized oligomer would have to be >4-fold that of leaky vesicles. The possibility that monomeric ATPase oligomerizes during activity assays can be theoretically evaluated by considering the conditions of assay and what is currently known about the kinetics of protein–protein interactions. The solubilized preparation does not show any measurable time lag in achieving maximal ATPase velocity during assays. Therefore, substrate-induced oligomerization would have to be near completion (≥90%) within the 5–10-s mixing period prior to the recording of activity. If we consider a dimer to be the minimal functional unit and assume a simple second-order model of dimerization (Gutfreund, 1972), we conservatively estimate that the second-order diffusional rate constant for the monomer–monomer interaction would have to be $>10^6$ M^{-1} s^{-1} to prevent production of a time lag in the activity recording. This rate is beyond the currently accepted limits for diffusion-limited protein–protein interactions (Gutfreund, 1972).

Active enzyme centrifugation analysis provides a direct assay of the molecular size of the active species. This method is particularly sensitive for the detection of the largest active particle. The $C_{12}E_8$-solubilized dimer of Ca^{2+}-ATPase is believed to have an $s_{20,w}$ value of 8–9 S (le Maire et al., 1978). A significantly heterogeneous population of active monomers and oligomers would have manifested itself as multiplicity of bands or produced a clear trend toward increased skewness of the activity bands during the course of an AEC experiment. Within the limits of the analysis, the symmetry and single component shape of the activity bands indicate that this solubilized preparation contains only one active species.

Sedimentation equilibrium of the total protein (A_{280}) indicates that within 24 h of solubilization <20–30% of the preparation exists as an oligomer, best described as a tetramer. Continued storage of the preparation leads to more extensive aggregation. The initial tetrameric species may represent incompletely solubilized, undissociated enzyme since Ca^{2+}-ATPase in SR vesicles often appears to be tetrameric (Vanderkooi et al., 1977; Pick & Racker, 1979; Scales & Inesi, 1976). Alternatively, the tetramer may be the beginning of the more extensive aggregation which follows with storage. The aggregated forms of the protein do not sediment as active species, as discussed above, and are most likely comprised of inactive units since the specific activity of the preparation also decreases with storage. However, it is possible that some of the aggregated units *dissociate* to active monomers during active enzyme centrifugation as a result of either dilution or substrate-induced *dissociation.*

The above diffusional rate constant calculations minimally suggest that a proposed substrate-dependent equilibrium between monomer and oligomer would have to occur over a much shorter time span than that of a sedimentation velocity experiment. At any particular protein concentration, it is not possible by active enzyme sedimentation either to detect a rapid monomer ↔ oligomer equilibrium or to determine which species of that equilibrium is active (Llewellyn & Smith, 1978). The obtained $\bar{s}$ value would be a weighted average of the sedimentation coefficients of the species at equilibrium, dependent upon protein concentration and the equilibrium constant. (The same limitations apply to molecular sieve chromatography in the presence of substrates.) If such an equilibria existed, a change in protein concentration would result in a change in the observed $\bar{s}$. Activity sedimented with a constant rate over a 6-fold protein concentration range. Therefore, within this concentration range, the active species of this solubilized and delipidated preparation does not behave as a reversibly associating system of monomers and oligomers. This does not preclude associating states at higher protein concentrations, but it does demonstrate that associated states are not required for ATPase activity.

The molecular weight and dimensions of a sedimenting particle can be obtained from sedimentation data by using the diffusion constant (eq 4). We obtained an approximate $D_{20,w}$ from active enzyme centrifugation data which statistically overlapped with that reported for noncycling monomeric Ca^{2+}-ATPase in $C_{12}E_8$ (le Maire et al., 1978). An error of ±10% can be expected in the determination of D from AEC data (Cohen et al., 1967), and experimentally, our data had a greater error (±20%). It is noteworthy, however, that six out of seven AEC experiments yielded $D_{20,w}$ values above the range reported for noncycling enzyme. It is intriguing to consider that these data suggest there may be a real difference in particle size between cycling and noncycling monomers. Ca^{2+}-ATPase exists in at least two conformational states (E and E′) during its enzymic cycle (de Meis & Vianna, 1979). Even a small conformational change in the protein during enzymatic cycling could result in altered levels of detergent binding and thus change the particle Stokes radius (Tanford et al., 1974). A change in detergent binding would also be consistent with observed losses in activity during cycling. We (data not shown) and others (Andersen et al., 1982) have concluded that this decrease in activity is due to a destabilized E′ conformation of the $C_{12}E_8$-solubilized enzyme. The noncycling enzyme is generally stabilized into the E conformation by saturating concentrations of Ca^{2+}. A smaller particle size for cycling enzyme would be consistent with the E′ conformation having a reduced level of $C_{12}E_8$ binding. However, differences in particle shape between the cycling and noncycling enzyme may arise directly from protein conformational changes. Recent data indicate that a substantial structural change occurs in vesicular Ca^{2+}-ATPase upon induction of enzyme cycling by the addition of ATP and Ca^{2+} (Watanabe & Inesi, 1982). Further structural studies on cycling and noncycling enzymes will be needed to fully appreciate the significance of these observations.

Using $s_{20,w}$ and $D_{20,w}$ obtained from active enzyme centrifugation and δ_d obtained with noncycling enzyme, we calculate an M_p which falls within the reported range for monomeric Ca^{2+}-ATPase. A reduction in δ_d for the cycling enzyme still yields a value for M_p within the monomer molecular weight range. Even if we use the $D_{20,w}$ reported for noncycling enzyme, the M_p calculated from the active enzyme sedimentation rate constants can only be attributed to monomeric enzyme. The monomer must be ATPase active. These data leave two mechanistic options. Either the monomer possesses ATPase activity uncoupled from Ca^{2+} transport or the monomer is the minimal functional unit for ATPase activity and Ca^{2+} pumping.

Arguing in favor of the latter conclusion, we recently reported (Martin, 1982) that the monomer can exist in states

analogous to those of vesicular enzyme, specifically E, E′, E∼P, and E′–P, and that it can pass through these states reversibly with similar dependence on Ca^{2+} concentration. Others have shown that monomeric Ca^{2+}-ATPase maintains cooperative Ca^{2+} activation of ATPase activity (le Maire et al., 1978; Andersen et al., 1982; Murphy et al., 1982) indicating that such interactions are intramolecular. Additionally, it was recently demonstrated that there is only one protein unit per *active* ATP binding site in SR vesicles (Andersen et al., 1982).

The above experiments extend the application of active enzyme centrifugation to detergent-solubilized membrane proteins. Data analysis is directly analogous to methods developed with aqueous soluble proteins provided the effects of detergent and lipid binding are taken into account. This method offers distinct advantages for functional unit determinations over recently applied approaches of protein cross-linking and gel electrophoresis or column chromatography in the presence of substrate since in active enzyme centrifugation only the active species are monitored as opposed to the total protein.

Acknowledgments

I thank Dr. Joseph M. Corless for the use of his computer facilities and his assistance in programming the data analysis. I also thank Drs. Darrell R. McCaslin and Jacqueline A. Reynolds for their many helpful discussions and Dr. Charles Tanford for critical review of the manuscript.

Registry No. ATPase, 9000-83-3; dodecyl octaethylene glycol monoether, 3055-98-9.

References

Andersen, J. P., Moller, J. V., & Jorgensen, P. L. (1982) *J. Biol. Chem. 257*, 8300–8307.

Bartlett, G. R. (1959) *J. Biol. Chem. 234*, 466–468.

Bevington, P. R. (1969) *Data Reduction and Error Analysis for the Physical Sciences*, McGraw-Hill, New York.

Brady, G. W., Fein, D. B., Harder, M. E., Spehr, R., & Meissner, G. (1981) *Biophys. J. 34*, 13–34.

Claverie, J. M. (1980) *Arch. Biochem. Biophys. 202*, 160–167.

Cohen, R., & Mire, M. (1971) *Eur. J. Biochem. 23*, 267–275.

Cohen, R., Giraud, B., & Messiah, A. (1967) *Biopolymers 5*, 203–225.

Craig, W. S. (1982) *Biochemistry 21*, 2667–2674.

Dean, J. A., Ed. (1979) in *Lange's Handbook of Chemistry*, 12th ed., pp 5–86, McGraw-Hill, New York.

Dean, W. L., & Tanford, C. (1978) *Biochemistry 17*, 1683–1690.

de Meis, L., & Vianna, A. L. (1979) *Annu. Rev. Biochem. 48*, 275–292.

Elder, J. P. (1979) *Methods Enzymol. 61*, 12–25.

Froehlich, J. P., & Taylor, E. W. (1976) *J. Biol. Chem. 251*, 2307–2315.

Gutfreund, H. (1972) *Enzymes: Physical Principles*, Wiley, New York.

Ikemoto, N., Garcia, A. M., Kurobe, Y., & Scott, T. L. (1981a) *J. Biol. Chem. 256*, 8593–8601.

Ikemoto, N., Miyao, A., & Kurobe, Y. (1981b) *J. Biol. Chem. 256*, 10809–10814.

Jorgensen, K. E., Lind, K. E., Roigaard-Petersen, H., & Moller, J. V. (1978) *Biochem. J. 169*, 489–498.

Kemper, D. L., & Everse, J. (1973) *Methods Enzymol. 27*, 67–82.

Kyte, J. (1981) *Nature (London) 292*, 201–204.

Lee, J. C., Gekko, K., & Timasheff, S. N. (1979) *Methods Enzymol. 61*, 12–25.

le Maire, M., Moller, J. V., & Tanford, C. (1976) *Biochemistry 15*, 2336–2342.

le Maire, M., Lind, K. E., Jorgensen, K. E., Roigaard, H., & Moller, J. V. (1978) *J. Biol. Chem. 253*, 7051–7060.

Llewellyn, D. J., & Smith, G. D. (1978) *Arch. Biochem. Biophys. 190*, 483–494.

Lowry, O. H., Roberts, N. R., Wu, M., Hixon, W. S., & Crawford, E. J. (1954) *J. Biol. Chem. 207*, 19–37.

Madeira, V. M. (1980) *Arch. Biochem. Biophys. 200*, 319–325.

Martin, D. W. (1982) *Ann. N.Y. Acad. Sci. 402*, 573–574.

Martin, D. W., & Tanford, C. (1981) *Biochemistry 20*, 4597–4602.

Meissner, G. (1975) *Biochim. Biophys. Acta 389*, 51–68.

Moller, J. V., Lind, K. E., & Andersen, J. P. (1980) *J. Biol. Chem. 255*, 1912–1920.

Murphy, A. J. (1976) *Biochem. Biophys. Res. Commun. 70*, 160–166.

Murphy, A. J., Pepitone, M., & Highsmith, S. (1982) *J. Biol. Chem. 257*, 3551–3554.

Nishimura, M., Ito, T., & Chance, B. (1962) *Biochim. Biophys. Acta 59*, 177–182.

Ottolenghi, P. (1975) *Biochem. J. 151*, 61–66.

Phillips, R. C., George, S. J. P., & Rutman, R. J. (1966) *J. Am. Chem. Soc. 88*, 2631–2640.

Pick, U., & Racker, E. (1979) *Biochemistry 18*, 108–113.

Pick, U., & Karlish, S. J. D. (1980) *Biochim. Biophys. Acta 626*, 255–261.

Remington, R. D., & Schork, M. A. (1970) *Statistics with Applications to the Biological and Health Sciences*, Prentice-Hall, Englewood Cliffs, NJ.

Rizzolo, L. J., le Maire, M., Reynolds, J. A., & Tanford, C. (1976) *Biochemistry 15*, 3433–3437.

Scales, D., & Inesi, G. (1976) *Biophys. J. 16*, 735–751.

Schechter, N. M., Sharp, M., Reynolds, J. A., & Tanford, C. (1976) *Biochemistry 15*, 1897–1904.

Shill, J. P., Peters, B. A., & Neet, K. E. (1974) *Biochemistry 13*, 3864–3871.

Tada, M., Yamamoto, T., & Tomomura, Y. (1978) *Physiol. Rev. 58*, 1–79.

Tanford, C. (1961) *Physical Chemistry of Macromolecules*, Wiley, New York.

Tanford, C., Nozaki, Y., Reynolds, J. A., & Makino, S. (1974) *Biochemistry 13*, 2369–2376.

Tanford, C., Nozaki, Y., & Rohde, M. F. (1977) *J. Phys. Chem. 81*, 1555–1560.

Taylor, B. L., Barden, R. E., & Utter, M. F. (1972) *J. Biol. Chem. 247*, 7383–7390.

Vanderkooi, J. M., Ierokomas, A., Nakamura, H., & Martonosi, A. (1977) *Biochemistry 16*, 1262–1267.

Verjovski-Almeida, S., & Inesi, G. (1979) *J. Biol. Chem. 254*, 18–21.

Vinograd, J., & Bruner, R. (1966) *Biopolymers 4*, 131–156.

Vinograd, J., Bruner, R., Kent, R., & Weigle, J. (1963) *Proc. Natl. Acad. Sci. U.S.A. 49*, 902–910.

Warren, G. B., Toon, P. A., Birdsall, N. J. M., Lee, A. G., & Metcalfe, J. C. (1974) *Proc. Natl. Acad. Sci. U.S.A. 71*, 622–626.

Watanabe, T., & Inesi, G. (1982) *Biochemistry 21*, 3254–3259.

Watanabe, T., Lewis, D., Nakamoto, R., Kurzmack, M., Fronticelli, C., & Inesi, G. (1981) *Biochemistry 20*, 6617–6625.

Wei, G. J., & Deal, W. C. (1979) *Biochemistry 18*, 1129–1137.